Getriebespezifische Schadensanalyse an elektromechanischen Antriebssystemen unter Verwendung mehrerer Beschleunigungssensoren und künstlich neuronaler Netze

Gearbox-specific failure analysis on electromechanical drive systems using multiple acceleration sensors and artificial neural networks

M. Eng. Timo König, M. Eng. Roman Bader, B. Eng. Suparshwa Pandit, Prof. Dr.-Ing. Markus Kley
Hochschule Aalen, Institut für Antriebstechnik Aalen, 73430 Aalen, timo.koenig@hs-aalen.de

Kurzfassung

In vielen Anwendungen in Produktionsumgebungen werden elektromechanische Antriebssysteme, die aus mehreren Getrieben bestehen, nicht zustandsorientiert gewartet. Die schlechter werdenden Anlagenzustände, die im Zusammenhang mit den jeweiligen Getriebezuständen stehen, können somit nicht erkannt und analysiert werden. Dies führt mit zunehmender Betriebsdauer zu einer Verminderung des Wirkungsgrads sowie im weiteren Sinne zu ungeplanten Fehlern und Ausfällen der Antriebseinheiten. Die Integration von Beschleunigungssensoren in die verbauten Getriebe bietet die Möglichkeit den Zustand der Antriebssysteme getriebespezifisch zu überwachen. Die Messungen werden unter Laborbedingungen sowohl an Getrieben im Neuzustand als auch an Feldrückläufern, die unter realen Bedingungen in Produktionsumgebungen eingesetzt sind, durchgeführt. Die relevanten Signalanteile in den erfassten Schwingungssignalen werden mit Hilfe einer Hüllkurvendemodulation hervorgehoben und mit einem künstlichen neuronalen Netz weiterverarbeitet, sodass eine getriebespezifische Schadensanalyse von Fehlerzuständen ermöglicht wird. Eine Optimierung der Hyperparameter des neuronalen Netztes ermöglicht eine bestmögliche Parameterabstimmung, sodass eine möglichst gute Performance des Algorithmus erreicht wird.

Abstract

In many applications in production environments, electromechanical drive systems consisting of several gearboxes are not maintained in a condition-oriented manner. The deteriorating system conditions, which are related to the respective gearbox conditions, can therefore not be recognised and analysed. With increasing operating time, this leads to a decrease of the efficiency and, in the broader sense, to unplanned errors and failures of the drive units. The integration of acceleration sensors in the installed gearboxes offers the possibility to monitor the condition of the drive systems in a gearbox-specific manner. The measurements are carried out under laboratory conditions on gearboxes in new condition as well as on field returns used under real conditions in production. The relevant signal components in the recorded vibration signals are highlighted with the help of an envelope demodulation and further processed with an artificial neural network, so that a gearbox-specific damage analysis of fault conditions is possible. An optimisation of the hyperparameters of the neural network enables the best possible parameter tuning so that the algorithm achieves the best possible performance.

1 Introduction

The gearboxes installed in electromechanical drive systems, which in this application are planetary and offset gearboxes, have an essential influence on the reliability of the overall system. According to the current state of the art, most drive systems from industrial practice are not maintained in a condition-oriented manner. This leads to unplanned failures as well as the replacement of components before the actual service life of the components is reached. Gearbox-specific condition monitoring on the drive systems using two acceleration sensors enables a damage detection on the installed gearboxes, so that the probability of failure of the entire drive system is reduced. A vibration-based monitoring of the drive system, the pre-processing of the acquired data with an envelope demodulation and a fast Fourier transform (FFT) as well as the damage detection with a multi-input feed-forward neural network is experimentally considered under laboratory conditions. The best possible tuning of the hyperparameters of the artificial neural network is achieved by optimising the parameters for better performance.

2 State of the art

The implementation of a condition monitoring system increases the reliability of gearboxes and drive systems. It is possible to use different status variables, such as the Root-Mean-Square, that allow conclusions to be drawn about the system status of the drive systems for status-oriented and status-based monitoring. Vibration analysis, which is to be implemented in the present application, offers the essential advantage that damage and faults in systems can be detected with a clear warning time. [1–3]

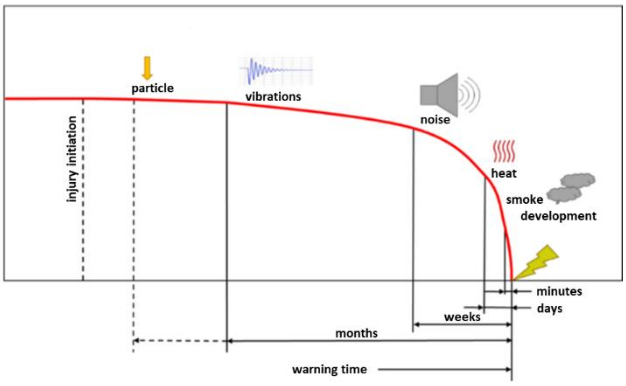

Figure 1: Damage progression as a function of time [1]

The mechanical components of electric motors, e.g. the roller bearings, can also be included in condition monitoring systems [4]. The generation of faulty system states sometimes requires very long operating times of the drive systems until a damage occurs. In reality, defective returns from field operation with a degraded overall state are therefore often used and compared with systems in a fault-free state [2, 5]. It is important to note that vibration measurements can be negatively influenced by the sensor positioning, external vibration excitation as well as the sensor performance [6–8]. The analysis of periodically occurring vibrations, which are caused by gear damage, for example, is often carried out using frequency domain analysis, as this offers the possibility of identifying the source of the faults [3]. The use of envelope analysis helps to reveal periodical excitations hidden in the raw vibration signal [9]. The calculation of condition indicators in the time and frequency domain also enables conclusions regarding component-specific faults and damages [10]. Following the conventional analysis methods, machine learning algorithms offer essential advantages in damage analysis and the detection of faulty conditions [11]. There are various feature extraction methods and machine learning algorithms for analysing sensor data in the context of machine fault detection, such as neural networks and support vector machines [12].
A paper shows that neural networks enable a classification-based analysis of acquired sensor data. It is also described that processing vibration and current signals with deep learning algorithms leads to better classification results in certain applications. Modern machines are complex in design, so it is important to focus on the vibrations caused by faulty parts rather than all the vibrations generated. [13]
A backpropagation neural network is also used for a classification based on the speed of a gearbox and oil-related gearbox faults. The use of calculated power spectrums results in refined signals to enable an improved feature extraction. The analysis of vibration signals provides important data on the condition of the system, fault detection as well as monitoring parameters. [14]

The state of the art describes existing methods of fault analysis on drive systems using conventional analysis methods as well as machine learning models. This work has similarities with various other publications. As a differentiation, however, it should be emphasised that a gearbox-specific fault analysis is carried out using faulty returns from field operation.

3 Data generation

The vibration data is generated on an electromechanical drive unit consisting of an electric motor, a planetary gear and an offset gear (Figure 2). Acceleration sensors are installed on each of the gearboxes so that gearbox-specific monitoring is possible. The planetary gearbox has a transmission ratio of $i_P = 24.92$ and the offset gearbox of $i_O = 1.5$. The tests are carried out at maximum speed of the drive unit.

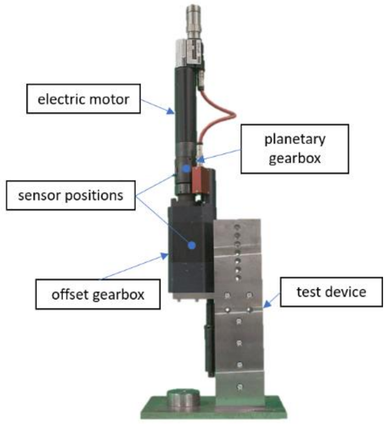

Figure 2: Test setup

The tests are carried out according to the test plan shown in Table 1. The prefix “P” represents the planetary gearbox and the “O” denotes the offset gearbox. The OK stands for a gearbox in a good condition and NOK for a gearbox in a bad condition (field return). The different test setups in Table 1 are realised by combining the different gearboxes with different system states. For this reason, assembling and disassembling of the drive units is necessary. The measurement duration per test is $t_S = 0{,}5\ s$ at a sampling frequency of $f_S = 25600\ Hz$.

Table 1: Test plan

test setup	Test-Nr. Sensor planetary gear [from - to]		Test-Nr. Sensor offset gear [from - to]	
1	P-OK-001	P-OK-096	O-OK-001	O-OK-096
	P-OK-097	P-OK-192	O-OK-097	O-OK-192
	P-OK-193	P-OK-288	O-OK-193	O-OK-288
2	P-NOK-001	P-NOK-096	O-NOK-001	O-NOK-096
	P-NOK-097	P-NOK-192	O-NOK-097	O-NOK-192
	P-NOK-193	P-NOK-288	O-NOK-193	O-NOK-288
3	P-OK-289	P-OK-384	O-NOK-289	O-NOK-384
	P-OK-385	P-OK-480	O-NOK-385	O-NOK-480
	P-OK-481	P-OK-576	O-NOK-481	O-NOK-576
4	P-NOK-289	P-NOK-384	O-OK-289	O-OK-384
	P-NOK-385	P-NOK-480	O-OK-385	O-OK-480
	P-NOK-481	P-NOK-576	O-OK-481	O-OK-576

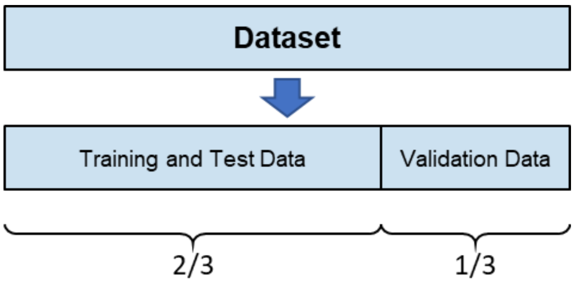

Figure 3: Training, test and validation data

The training and test data are extracted in relation to the validation data in a ratio of 2/3 to 1/3, as visualized in Figure 3. The last measurement series in each test setup (for example 193 to 288 for test setup 1) is used for validation. The training and test data are split randomly.

4 Model architecture

4.1 Experimental results

The spectrograms in Figure 4 show the amplitude levels of the envelope spectrums by FFT for both gears and both conditions depending on the measurement number. It should be noted that the upper bound of the colour scale for each gear type is limited to the mean value plus three times the standard deviation of all amplitudes. Thus, some extreme amplitudes get cut off, but the overall visibility of the most amplitudes at relevant frequencies is improved. Beginning and end of each data block for training/test and validation according to the measurement plan is highlighted in the spectrograms.

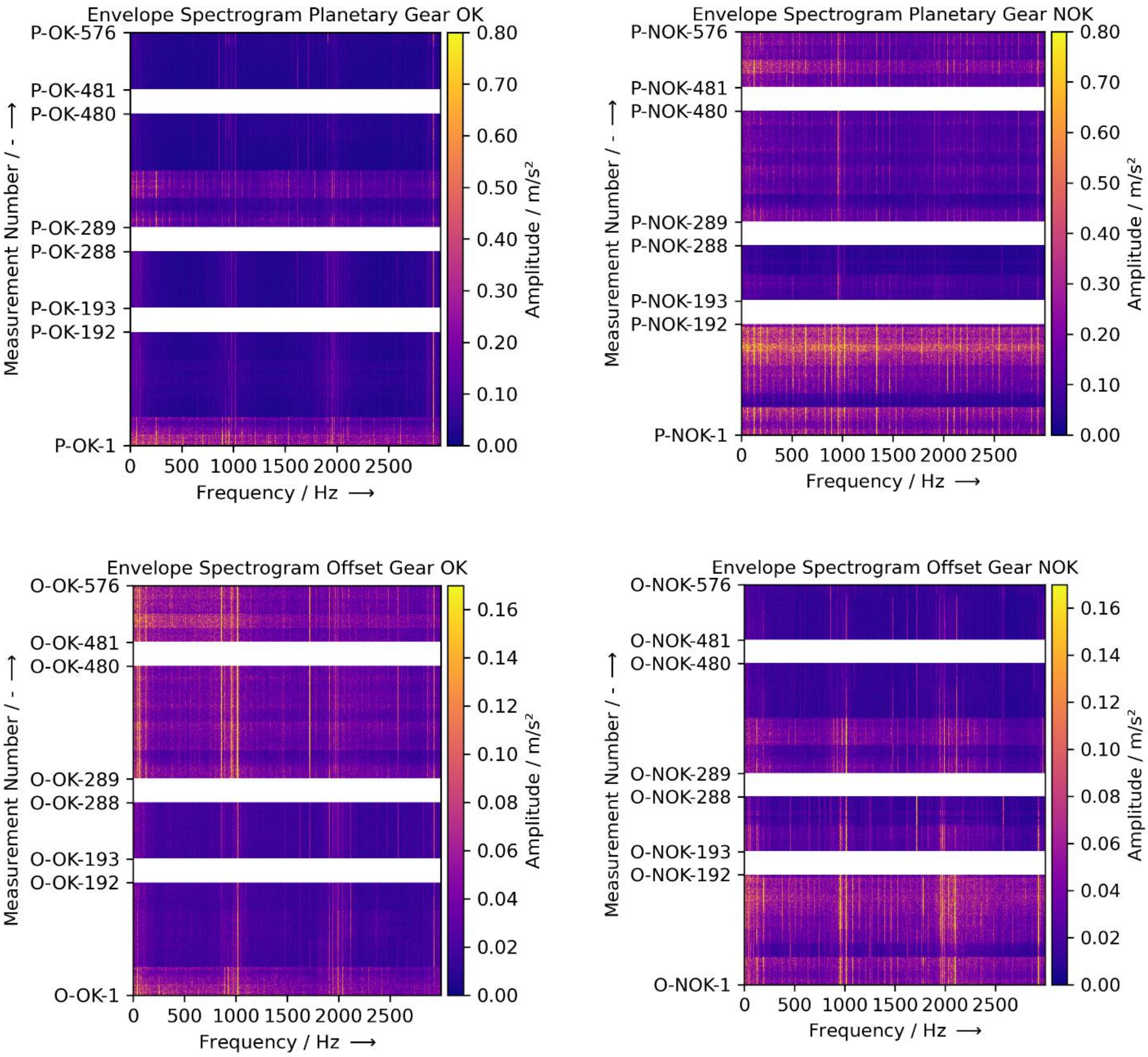

Figure 4: Spectrograms of the envelope signals of the planetary and the offset gearbox

Basically, for all four gearbox and condition combinations, it can be seen that the envelope spectra shown are not homogeneous across the measurement numbers. Despite the constant external operating conditions, fluctuations in both the amplitudes of significant frequencies and background noise are visible.

In the case of the planetary gear (prefix P), it can be seen that there is often a higher amplitude level in the NOK state than in the OK state, which is attributed to general wear. In addition, one can find some characteristic frequency lines in OK state, which are also visible in the NOK spectrogram. However, several distinctive characteristic frequencies, which are easily distinguishable in the NOK spectrogram, are not present in the OK state or have only low amplitudes. Overall, both states are also clearly differentiable from each other visually.

The offset gear (prefix O) differs from the findings above. Considerable noise and distinctive characteristic frequencies are present in the OK state as well as in the NOK state. There is significant inhomogeneity of the individual spectrums in the spectrograms. If - as in this case - no precise assignment of the individual fault frequencies is done, the OK and NOK states of the offset gear cannot be clearly distinguished. In general, the maximum amplitudes of the offset gear are lower than those of the planetary gear.

4.2 Multi-input neuronal network

A multi-input feed-forward neural network is used for condition classification. It consists of two separate input layers for the envelope spectrums of both sensors. The number of neurons per input layer is equal to the amount of discrete frequencies per spectrum. Each input layer is followed by a hidden layer, whose outputs are concatenated then. From now on, data of both sensors is processed together. This is done by another hidden layer and the subsequent application of a dropout function that prevents overfitting. The final output layer consists of two neurons that each represent the condition of one gearbox. Figure 5 shows the resulting structure of the neural network.

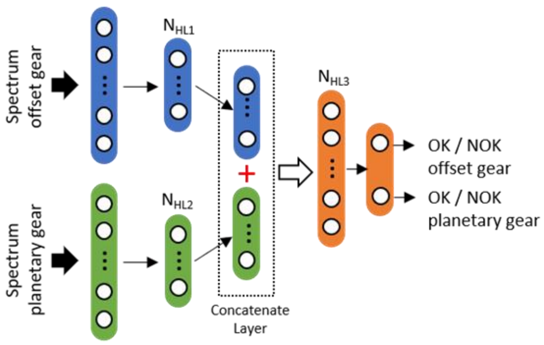

Figure 5: Structure of the neural network

Because a multi-label classification is implemented here, both neurons can have the value 0 or 1 independently from each other. 0 represents an OK gear, a value of 1 denotes a NOK gear. The real value of an output neuron is usually a decimal number between 0 and 1. If a user-defined threshold (here at 0.7) is exceeded, the decimal number is rounded up to 1, otherwise it is set to 0. The choice of threshold can significantly influence the classification.

While the number of neurons of the input and output layer is determined a priori by the number of input (each 2999) and output (2) values, the structure of the hidden layers is relatively freely selectable. However, the classification result often depends heavily on the choice of suitable parameters. Hyperparameter optimisation can be applied as a transparent method for selecting these parameters. In the present case, the number of neurons N_{HL1}, N_{HL2} and N_{HL3} of the respective hidden layers, the batch size and the dropout rate are determined by hyperparameter optimisation. It should be noted that the number of neurons for both N_{HL1} and N_{HL2} should be the same, which is ensured here via a constraint. A random search (see Figure 6) is performed on a predefined search space (see Table 2) with a maximum of 512 allowed iterations.

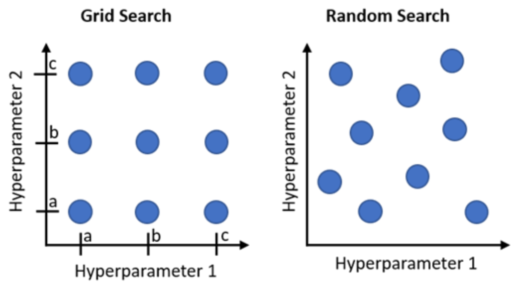

Figure 6: Hyperparameter optimisation

The validation accuracy of the neural network is considered as a criterion for the evaluation of the suitability of each parameter set. The absolute frequency distribution of the resulting validation accuracy during optimisation process is shown in Figure 7. It can be seen that several combinations provide a validation accuracy up to 100 %.

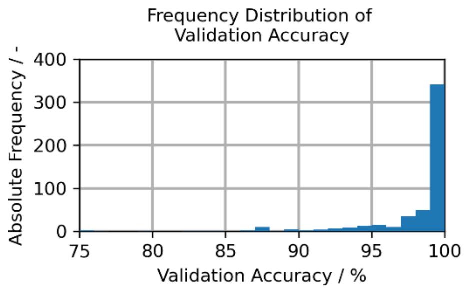

Figure 7: Absolute frequency of a validation accuracy during hyperparameter optimisation

The parameter combination shown in Table 2 was chosen for the final classification process. This choice was made based on good experience with similar configurations in previous examinations.

Table 2: Search space and chosen hyperparameter

	Optimised Hyperparameter	Selected Hyperparameter
Number of Neurons Hidden Layer 1 and 2	$N_{HL1} = N_{HL2} =$ {32, 64, 128, 256}	$N_{HL1} = N_{HL2} = 64$
Number of Neurons Hidden Layer 3	N_{HL3} = {8, 16, 32, 64}	$N_{HL3} = 16$
Dropout Rate	(0.1, 0.25)	0.17
Batch Size	{16, 32}	16

4.3 Algorithm performance

The training of the neural network over 256 epochs with a learning rate of 10^{-4} leads to a steadily decreasing loss function (Figure 9) when using training and test data. The global course of training and test accuracy (Figure 8) is monotonically increasing and converges to 1 (100 %).

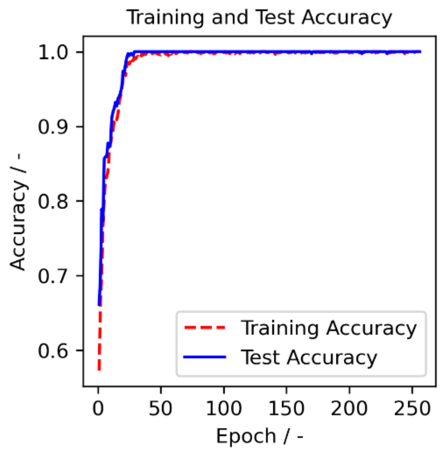

Figure 8: Accuracy of the train and test

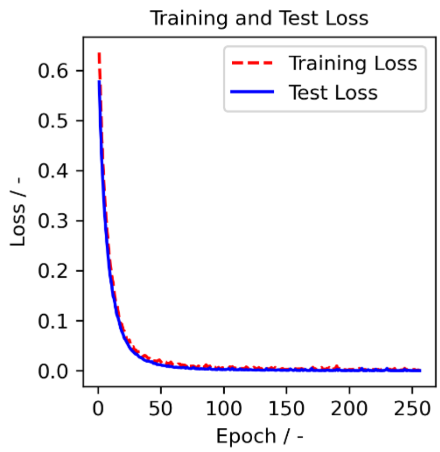

Figure 9: Loss function of the train and test

Minor deviations could be related to the random selection of the training and test data. The subsequent prediction of the system state by using the validation data results in a validation accuracy of 100 % for the planetary gear and 98 % for the offset gear (see matrices in Figure 10).

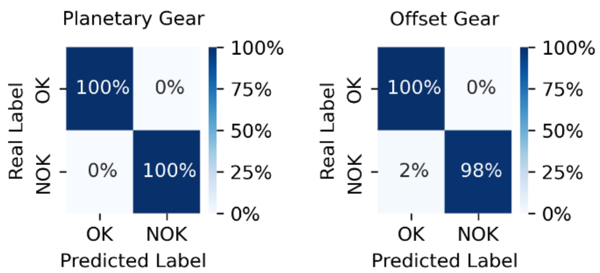

Figure 10: Confusion matrices of the validation accuracy

The system conditions OK and NOK can be well differentiated by the algorithm. This justifies the usage of a neural network especially because of the difficult (visual) distinctiveness regarding the offset gearbox condition (see 4.1).

5 Summary and outlook

In summary, artificial neural networks significantly improve the fault detection performance of envelope spectra. Inhomogeneous unclear frequency patterns can be classified with satisfactory accuracy. The generalisation of the algorithm to a wider range of good and damaged gearboxes and its sensitivity to different degrees of damage are open questions to be considered in future work.

Funding Acknowledgements

This work is supported by VDI/VDE Innovation + Technik GmbH as the project management organisation of the Federal Ministry for Economic Affairs and Energy within the context of a ZIM cooperation project under the funding code 16KN088821.

References

[1] Schaeffler Technologies, *Wälzlagerpraxis: Handbuch zur Gestaltung und Berechnung von Wälzlagerungen,* 5th ed. Mainz am Rhein: Vereinigte Fachverlage, 2019.

[2] T. König, R. Bader, and M. Kley, “Schwingungsbasierte Fehlererkennung und Schadensdetektion an Getrieben durch Einbindung von Methoden des Machine Learning,” *3. VDI-Fachtagung Schwingungen 2021*, pp. 53–66, 2021, doi: 10.51202/9783181023914-53.

[3] Schaeffler Technologies, *Condition Monitoring Praxis: Handbuch zur Schwingungs-Zustandsüberwachung von Maschinen und Anlagen,* 1st ed. Mainz am Rhein: Vereinigte Fachverlage, 2019.

[4] D. Proksch, L. Stütz, J. Krotsch, B. Höfig, and M. Kley, “Development of a Digital Twin for an Induction Motor Bearing Voltage Simulation,” *2021 IEEE Jordan International Joint Conference on Electrical Engineering and Information Technology (JEEIT)*, pp. 103–107, 2021, doi: 10.1109/JEEIT53412.2021.9634143.

[5] J. Deckers and B. Back, “Getriebediagnose 4.0 – Herausforderungen bei der Nutzung künstlicher Intelligenz im schwingungsbasierten Condition Monitoring,” *2. VDI Fachtagung Schwingungen*, pp. 189–200, 2019, doi: 10.51202/9783181023662-189.

[6] M. Bauer, F. Wagner, and M. Kley, “Optimierung der Sensorpositionierung bei schwingungsbasierter Wälzlagerzustandsüberwachung unter Einbezug von Systemeigenmoden,” *tm - Technisches Messen*, vol. 88, no. 11, pp. 674–685, 2021, doi: 10.1515/teme-2021-0045.

[7] M. Bauer, M. Hoffmann, and M. Kley, “Methode zur Erkennung des Einflusses von äußeren Schwingungsanregungen bei der

Wälzlagerzustandsüberwachung," *2. VDI Fachtagung Schwingungen*, pp. 343–354, 2019, doi: 10.51202/9783181023662-343.

[8] M. Bauer, D. Proksch, J. Kopetschek, F. Wagner, and M. Kley, "Entwicklung und Validierung einer Methode zur Ermittlung der minimalen Performanceanforderungen an Sensoren für die schwingungsbasierte Zustandsüberwachung," *3. VDI Fachtagung Schwingungen*, pp. 89–104, 2021, doi: 10.51202/9783181023914-89.

[9] R. B. Randall, *Vibration-based condition monitoring: Industrial, automotive and aerospace applications,* 2nd ed. Hoboken, NJ: Wiley, 2021.

[10] V. Sharma and A. Parey, "A Review of Gear Fault Diagnosis Using Various Condition Indicators," *Procedia Engineering*, vol. 144, pp. 253–263, 2016, doi: 10.1016/j.proeng.2016.05.131.

[11] D. K. Appana, A. Prosvirin, and J.-M. Kim, "Reliable fault diagnosis of bearings with varying rotational speeds using envelope spectrum and convolution neural networks," *Soft Computing*, vol. 22, no. 20, pp. 6719–6729, 2018, doi: 10.1007/s00500-018-3256-0.

[12] S. R. Saufi, Z. A. B. Ahmad, M. S. Leong, and M. H. Lim, "Challenges and Opportunities of Deep Learning Models for Machinery Fault Detection and Diagnosis: A Review," *IEEE Access*, vol. 7, pp. 122644–122662, 2019, doi: 10.1109/ACCESS.2019.2938227.

[13] G. Jiang, J. Zhao, C. Jia, Q. He, P. Xie, and Z. Meng, "Intelligent Fault Diagnosis of Gearbox Based on Vibration and Current Signals: A Multimodal Deep Learning Approach," *019 Prognostics and System Health Management Conference (PHM-Qingdao)*, pp. 1–6, 2019, doi: 10.1109/PHM-Qingdao46334.2019.8942903.

[14] T. W. Waqar, M. Demetgul, and C. Kelesoglu, "Fault Diagnosis on Bevel Gearbox with Neural Networks and Feature Extraction," *Elektronika ir Elektrotechnika*, vol. 21, no. 5, 2015, doi: 10.5755/j01.eee.21.5.13334.

DOI: 10.17185/duepublico/75428
URN: urn:nbn:de:hbz:465-20220222-162635-2